EXPERIMENTAL VALIDATION OF A LINEAR NUMERICAL MODEL FOR THE WATER WAVE SCATTERING BY A COMPLIANT FLOATING DISK

F. Montiel[†,*], **F. Bonnefoy**[‡], **L. G. Bennetts**[†], **V. A. Squire**[†], **P. Ferrant**[‡], **P. Marsault**[‡]
[†]Department of Mathematics and Statistics, University of Otago, Dunedin, New Zealand
[‡]Laboratoire de Mécanique des Fluides, École Centrale de Nantes, Nantes, France.
[*]Email: fmontiel@maths.otago.ac.nz

Talk Abstract

A series of wave tank experiments were recently conducted at École Centrale de Nantes in France to validate the linear scattering theory used to model hydroelastic interactions between regular water waves and sea-ice floes. The experiments discussed in this paper are those involving a single compliant disk. This was set in motion by a controlled incident wave train, generated by a wavemaker. The deflection of the disk was recorded by an optical motion tracking device and the scattered waves around the disk were measured with resistive wave gauges. The disk was only allowed to move in heave, roll and pitch, in addition to the flexural response. The restrictions are in accord with those of the linear model. Aspects of the technical solutions and the measurement devices used in the experiments are described. Preliminary comparative numerical versus experimental results are also presented.

Introduction

In the polar seas the marginal ice zone (MIZ) exists as an interfacial region between the open ocean and the quasi-continuous interior ice cover. It is composed of a distribution of separate sea-ice floes, which either form in place or are advected into the zone from adjacent frozen seas, but its morphology is shaped mainly by the wave-induced breakup of its constituent floes. The primary source of ocean wave attenuation in the MIZ is believed to be due to the scattering that occurs when a wave interacts with a floe. These scattering processes have been studied extensively in the field of hydroelasticity, mostly with linear numerical models, but the lack of experimental data is impeding this research area.

Models of large ice fields are built up from the responses of individual floes. The theoretical side of this research is now well developed and a comprehensive synthesis can be found in [1]. However, very few laboratory experiments have been performed to study water wave scattering by an elastic floe. The most relevant study was conducted in Japan by S. Sakai and K. Hanai in a wave flume, using polyethylene sheets as a substitute for sea-ice. Their data were utilised by [2], who compared the response of these elastic sheets with a two-dimensional linear model. The comparisons made for a single sheet showed that an increasing agreement was found as the frequency decreased, although the frequencies used correspond to wavelengths significantly smaller than the sheet's length.

In the current paper, we present the series of laboratory experiments that were recently performed by the authors in a wave basin at the Department of Ocean Engineering of École Centrale de Nantes. These experiments represent the first attempt to record the response of a compliant floating disk to linear water waves in a three-dimensional setting, and therefore supersede the previous experiments described by [2]. They are hoped to provide a benchmark data set. Specifics on the experimental facilities and measurement devices are given. We also discuss the technical configuration designed to reproduce the conditions assumed in the numerical model.

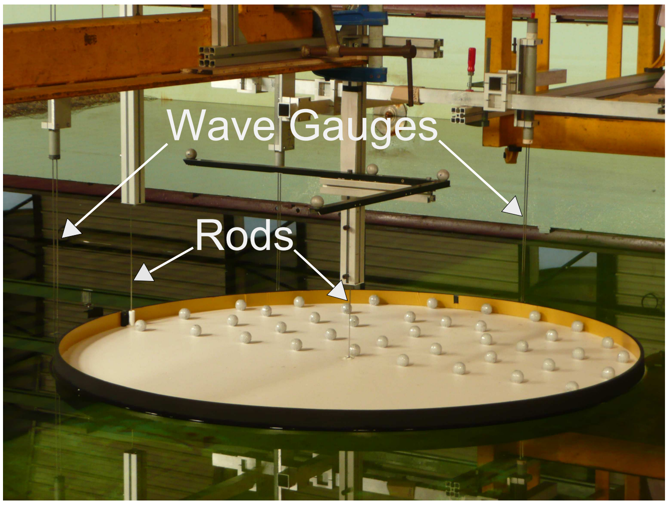

Figure 1: Fully equipped 10 mm-thick disk

Experimental Setup

Facilities

The wave tank used for the experiments is 15.5 m long, 9.5 m wide and 1.9 m deep. A hinged-flap wavemaker, composed of two parallel and connected flaps, generates uni-directional waves for a range of amplitudes and wavelengths, which may be adapted to the linear wave conditions sought. An absorbing beach is located at the opposite side of the basin. Its coefficient of reflection has been evaluated experimentally by [3], and varies between 5 and 13% for the different study cases considered.

The waves interact with a disk made of expanded PVC. This material was chosen because it has density and flexural rigidity that, when scaled, are comparible to sea-ice.

Three disks with different thicknesses were used for the experiments. The thicknesses were 3, 5 and $10\,\mathrm{mm}$ and each disk had a radius of $0.72\,\mathrm{m}$. The Young's moduli were measured with a 4-point bending test. Their values were 838, 503 and $496\,\mathrm{MPa}$, respectively for the 3, 5 and $10\,\mathrm{mm}$ disks.

Technical Setup

As the numerical model does not allow the disk to respond in surge, sway and yaw, a simple device composed of two vertical aluminium rods was developed to restrict these motions in the experimental setup. A rod of diameter 3 mm runs through the centre of disk so that surge and sway are reduced (the worst case being 3 mm). The friction resulting from the dynamical contact between the disk and the rod is minimised by enlarging the hole and screwing thin aluminium plates on each side of the disk. A second rod, of diameter 5 mm, runs through the disk close to an edge, so the rotation of the plate is limited to, at most, 1.5 degrees. The rods are visible in Figure 1. They are maintained by a rail structure fixed to a bridge platform that runs above the wave tank.

A series of tests performed prior to the experiments revealed the presence of green water loads under certain wave conditions. We eliminated this problem by adding a barrier to the edge of the disk. The barrier was made of a strip of neoprene foam, which was stuck around the disk, and was chosen for its low mass, waterproof and high ductility properties.

Measurement Devices

The originality of the present experiment resides in the recording of the wave induced deformations of a thin floating elastic body. An optical motion tracking device was employed to capture the deflection of the disk. This consisted of 39 polystyrene spherical markers, covered with a retro-reflective tape, which were placed over half the disk (see Figure 1); symmetry being assumed for the other half. The motion of these markers is then recorded by three InfraRed cameras. Two of the cameras are located on the shore, about 4 m away from the floe with different angles while the third one is fixed to the bridge

Figure 2: Camera fastened to the bridge and pointing down to the disk

above the disk and points downwards. Figure 2 shows the latter in a wide angle shot of the experimental setup. An accurate calibration of the device is required and average residues of 0.5–1 mm were achieved.

It is also of interest to measure the diffracted wave field. We recorded the wave height around half the disk (again symmetry is assumed) using five resistive wave gauges (see Figure 1). These were located at 45 degree intervals, and 0.22 m away from the disk's edge. The gauges provide measurements to an accuracy of less than 1 mm.

Study Cases Considered

A range of wave conditions were tested for each of the three disks considered. The wave steepness, defined as the product of twice the wave amplitude divided by the wavelength, had to be small as we intended to compare the results with a linear model. We performed the experiments with two steepnesses, namely $\epsilon = 1\%$ and $\epsilon = 2\%$. For each case, a range of eight frequencies was studied, in the interval $f = 0.6$–1.3 Hz. Table 1 defines the different wave conditions generated for each floe, with wavelengths λ and amplitudes a_1 ($\epsilon = 1\%$) and a_2 ($\epsilon = 2\%$).

Table 1: Wave conditions

f(Hz)	0.6	0.7	0.8	0.9	1	1.1	1.2	1.3
λ(m)	4.3	3.2	2.4	1.9	1.6	1.3	1.1	0.9
a_1(mm)	22	16	12	10	8	7	5	5
a_2(mm)	43	32	24	19	16	13	11	9

To extract the scattered wave from the total wave height measured by the gauges, we ran the same range of tests without the disk. The incident wave was recorded so that the scattered wave component could be obtained by subtraction of the incident wave from the total wave measured with a disk present.

Numerical Model

For the numerical model, we consider a fluid domain Ω that is unrestricted in the horizontal directions and of finite depth, H say. Points in this domain are denoted $\mathbf{x} = (r, \theta, z)$, where z points upwards, with its origin coinciding with the undisturbed free surface. The origin of the radial coordinate, $r = 0$, is the centre of the disk, which is of thickness h. The incident wave travels in the direction $\theta = 0$. Let $d = h\rho/\rho_0$ be the Archimedean draught of the disk, where ρ and ρ_0 respectively are the density of the disk and the water.

Under the regular assumptions of linear wave theory, and assuming time-harmonic conditions of radian frequency ω, let the fluid motion be defined by the velocity potential $\Phi(\mathbf{x}, t) = \Re\mathrm{e}\left\{\phi(\mathbf{x})\,\mathrm{e}^{\mathrm{i}\omega t}\right\}$, where $\phi(\mathbf{x})$ is a complex scalar field. It satisfies Laplace's equation, $\Delta\phi = 0$, for all $\mathbf{x} \in \Omega$ and the no-flow condition $\partial_z\phi = 0$ at $z = -H$. On the free surface the linearised condition $\partial_z\phi = \alpha\phi$ applies, where $\alpha = \omega^2/g$, with $g \approx 9.81\,\mathrm{ms}^{-2}$ the acceleration due to gravity. In addition, the Sommerfeld radiation condition must be applied to ϕ in the far field $r \to \infty$.

The deformation of the disk is assumed to be characterised by the thin elastic plate theory. Consequently, the disk's response is completely described by its vertical oscillations. No surge, sway and yaw rigid body motions are considered. The hydrodynamic pressure acting on the disk's underside, at $z = -d$, can be expressed as the sum of an inertial term and a fourth order flexural term. Applying Bernoulli's equation gives

$$\left(\beta\nabla^4 + 1 - \alpha d\right)\partial_z\phi = -\alpha\phi, \tag{1}$$

where β is a scaled versions of the disk's flexural rigidity. Free motion is also assumed so at its edge the disk experiences no shearing stress and bending moment.

We seek separation solutions in both the open water region and the disk-covered region, and obtain a dispersion relation in each region. The dispersion relation in the free surface domain is

$$k \tan kH = -\alpha, \tag{2}$$

and is solved for the wavenumbers k. In the disk-covered region the dispersion relation is

$$\left(\beta\kappa^4 + 1 - \alpha d\right)\kappa \tan \kappa(H - d) = -\alpha, \tag{3}$$

and is solved for the wavenumbers κ. Equations (2) and (3) both have a single purely imaginary root that supports travelling waves and an infinite number of real roots that support evanescent waves. Additionally, Equation (3) has two complex conjugate roots associated with oscillating waves that decay exponentially. The radial dependence of the motion is given by modified Bessel functions, so that circular waves are scattered by the disk and decay geometrically with distance.

In a similar manner to [4], the expansions in both regions are then matched at the disk's edge to enforce continuity of fluid pressure and velocity. Inner-products are taken over the water column and the solution of the resulting system of equations is computed straightforwardly.

Preliminary Results

The motion tracking data provide the positions of each marker in the time domain, while the numerical model produces a steady state excitation of the disk at a given frequency. Consequently, special care must be taken in defining a relevant steady state of the disk's motion in the experiments. Assuming the system is slightly underdamped, the disk reaches the steady state quickly after the wave front has passed, but the response becomes rapidly contaminated by the waves that hit the disk after reflection against the side walls and the beach. Consequently the steady state is defined by a short temporal window that starts after the incident wave front has passed and ends before the reflected waves hit the disk. A moving-window Fourier tranform procedure is performed to extract the required amplitudes at the incident wave frequency, acting as a filter for the higher-order harmonics that are also captured.

A comparison of the disk's flexural response is the primary focus of the present analysis. We therefore write the displacement of the disk, $\eta(r, \theta)$, as the sum of the rigid body motions (roll neglected due to symmetry) plus a flexural term such that

$$\eta(r, \theta) = A_0 + A_1 r\cos\theta + \mathcal{F}(r, \theta), \tag{4}$$

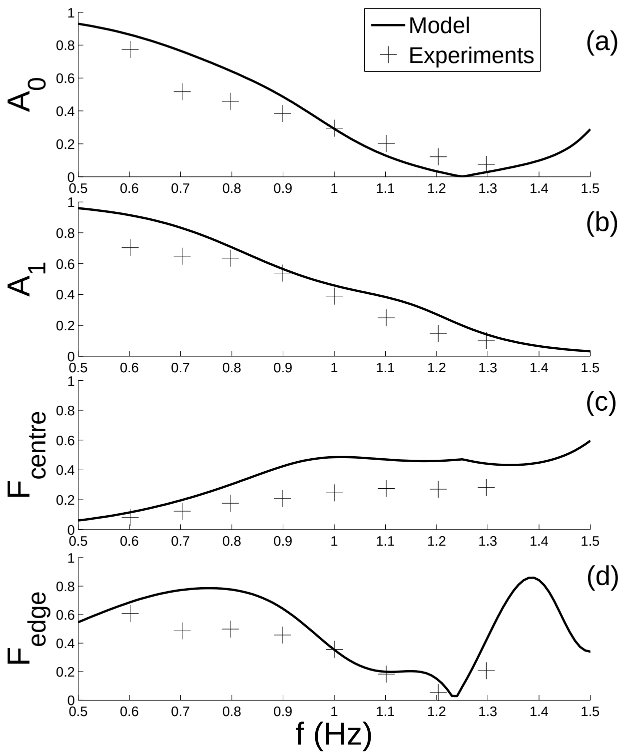

Figure 3: Model/experiments comparison of the scaled (a) heave coefficient A_0, (b) pitch coefficient A_1, and the flexurally-induced displacement of (c) marker 1 and (d) marker 2.

where A_0 is the heave, $A_1 r\cos\theta$ the pitch and $\mathcal{F}(r,\theta)$ the flexural term. The heave and pitch coefficients, A_0 and A_1, are given by

$$A_0 = \frac{1}{\pi R^2}\int_0^{2\pi}\int_0^R \eta(r,\theta)\, r\,\mathrm{d}r\,\mathrm{d}\theta, \tag{5}$$

$$A_1 = \frac{4}{\pi R^4}\int_0^{2\pi}\int_0^R \eta(r,\theta)\,(r\cos\theta)\; r\,\mathrm{d}r\,\mathrm{d}\theta. \tag{6}$$

In Figures 3a-b, the coefficients A_0, scaled by the incident wave amplitude, and A_1, scaled by the product of incident wave amplitude and wavenumber, are plotted against wave frequency for a floe of thickness $h = 5$ mm and incident waves of steepness $\epsilon = 1\%$. The comparison between experimental data (pluses) and numerical results (solid lines) shows a good qualitative agreement. The heave coefficient (Figure 3a) is overestimated by the model at low frequency, while for $f > 1\,\mathrm{Hz}$, the model underestimates the response. A resonance in heave, not shown in Figure 3a, occurs at $f = 1.55\,\mathrm{Hz}$ and the response then tends to zero as f increases. Figure 3b shows that the model narrowly overestimates the pitch response for the frequency range plotted, with a better agreement for mid-range frequencies.

A comparison between theory and experiments of the flexural response, $\mathcal{F}$, scaled by the incident wave amplitude is shown in Figures 3c-d, for two points on the disk. Figure 3c displays the scaled flexurally-induced displacement of the closest marker to the centre of the disk ($r = 30$ mm, $\theta = \pi/2$), marker 1 say, denoted F_{centre}. Figure 3d shows the flexurally-induced displacement of the closest marker to the front edge, located on the main diagonal with respect to the the direction of propagation of the incident wave ($r = 641$ mm, $\theta = 0$), marker 2 say, denoted F_{edge}. The comparison made in Figure 3c shows some dicrepancies, especially at high frequency. On the other hand, Figure 3d shows a good agreement at high frequency. In particular the phase change occuring between 1.2 and $1.3\,\mathrm{Hz}$ is present in both theory and experiments. For lower frequencies, the model overestimates the response, a feature that is present throughout this analysis.

Good agreement was normally found between numerical results and experimental data. The differences occuring at low frequencies suggest that other physical effects are important when the wavelength becomes larger than the disk's diameter. Furthermore, it is important to note that the experimental results produced in Figure 3 are only reliable up to the resolution of the measurement devices. We are aware that in certain cases the amplitudes measured have an order of magnitude similar to these resolutions, which means that large error bounds would apply. The experimental setup may also cause some discrepancies, especially in the vicinity of the centre of the disk. In particular, the friction caused by the contact between the rod and the disk could be restricting the vertical motion.

References

[1] Squire V. A., "Of ocean waves and sea-ice revisited", Cold Reg. Sci. Technol., 49, 110–133, 2007.

[2] Kohout A. L., Meylan M. H., Sakai S., Hanai K., Leman P. and Brossard D., "Linear water wave propagation through multiple floating elastic plates of variable properties", J. Fluids Struct., 23 , 649–663, 2007.

[3] Marsault P., "Étude expérimentale des interactions houle-glace de mer", Masters Thesis, 2010.

[4] Peter M. A., Meylan M. H. and Chung H., "Wave scattering by a circular elastic plate in water of finite depth: a closed form solution", Int. J. Offshore Polar Eng., 14, 81–85, 2003.